

**Resonant and nonresonant contributions to the weak  
 $D \rightarrow Vl^+l^-$  decays****S. Fajfer<sup>a</sup>, S. Prelovšek<sup>a</sup> and P. Singer<sup>b</sup>***a) J. Stefan Institute, Jamova 39, P. O. Box 300, 1001 Ljubljana, Slovenia**b) Department of Physics, Technion - Israel Institute of Technology, Haifa  
32000, Israel***ABSTRACT**

The Cabibbo suppressed decays  $D \rightarrow Vl^+l^-$  ( $V$  is light vector meson) present in principle the opportunity to observe the short distance FCNC transition  $c \rightarrow ul^+l^-$ , which is sensitive to physics beyond the Standard Model. We analyze these as well as the Cabibbo allowed  $D \rightarrow Vl^+l^-$  decays within the Standard Model, where in addition to the short distance dynamics also the long distance dynamics is present. The long distance contribution is induced by the effective nonleptonic weak Lagrangian accompanied by the emission of a virtual photon, which occurs resonantly via conversion from a vector meson  $\rho^0$ ,  $\omega$  or  $\phi$  or nonresonantly as direct emission from a  $D$  meson. We calculate the branching ratios for all  $D \rightarrow Vl^+l^-$  decays using the model, which combines heavy quark symmetry and chiral perturbation theory. The short distance contribution due to  $c \rightarrow ul^+l^-$  transition, which is present only in the Cabibbo suppressed decays, is found to be three orders of magnitude smaller than the long distance contribution. The branching ratios well above  $10^{-7}$  for Cabibbo suppressed decays could signal new physics. The most frequent decays are the Cabibbo allowed decays, which are expected at the rates, that are not much lower than the present experimental upper limit:  $D_s^+ \rightarrow \rho^+ \mu^+ \mu^-$  is expected at the branching ratio of approximately  $3 \cdot 10^{-5}$ , while  $D^0 \rightarrow \bar{K}^{*0} \mu^+ \mu^-$  is expected at  $1.7 \cdot 10^{-6}$ .

## I. INTRODUCTION

In the charm sector phenomena like  $D^0 - \bar{D}^0$  mixing, CP-violation and rare decay probabilities are small, which makes them good candidates as probes for new physics with small background from the Standard Model [1, 2, 3]. In particular, decays of type  $D \rightarrow Xl^+l^-$  were singled out [4, 5, 6] as a possible good window to non-standard contributions of the flavour-changing neutral transition (FCNC)  $c \rightarrow ul^+l^-$ , at the  $10^{-7}$  level for the branching ratios. This suggestion was prompted by the smallness of the short-distance (SD)  $c \rightarrow ul^+l^-$  contribution within the Standard Model, which leads [4, 6] to a branching ratio of only  $10^{-9}$  for the inclusive process. Although QCD corrections to this process have not been calculated in detail yet, these are not expected to affect significantly the size of the  $c \rightarrow ul^+l^-$  amplitude, as explained in the next section. Accordingly, one expects the hadronic exclusive decays induced by this SD transition to occur with branching ratios of the order of  $10^{-10}$ .

Further studies, which have considered the long-distance (LD) contribution to  $D \rightarrow Pl^+l^-$  transitions ( $P$  is light pseudoscalar) [6, 7] have concluded that these are larger than SD ones. The analysis of the LD contributions in  $D^{+,0} \rightarrow \pi^{+,0}l^+l^-$  [7] has shown these modes are expected to lead to branching ratios of the order of  $10^{-6}$  in the resonance region and a few times  $10^{-7}$  in the nonresonant region, thus practically invalidating their use for observing the  $c \rightarrow ul^+l^-$  transition within the Standard model.

A similar situation holds in the case of  $D \rightarrow V\gamma$  ( $D \rightarrow P\gamma$  is forbidden), where long distance effects [8, 9, 10] cause these modes to have branching ratios in the  $10^{-7} - 10^{-4}$  range. On the other hand, the SD component due to the magnetic electroweak penguin transition  $c \rightarrow u\gamma$  is GIM suppressed and does not reach beyond the  $10^{-9}$  range at most, despite of being considerably enhanced by QCD corrections [8, 11]. Thus, here again the LD effects mask the contribution of the SD  $c \rightarrow u\gamma$  loop, except for very special circumstances, which were pointed out recently [9, 12].

We analyze LD and SD contributions to all  $D \rightarrow Vl^+l^-$  decays within the Standard Model. The SD contribution due to  $c \rightarrow ul^+l^-$  is present only in the Cabibbo suppressed decays  $D^0 \rightarrow \rho^0l^+l^-$ ,  $D^0 \rightarrow \omega l^+l^-$ ,  $D^0 \rightarrow \phi l^+l^-$ ,  $D^+ \rightarrow \rho^+l^+l^-$  and  $D_s^+ \rightarrow K^{*+}l^+l^-$ . Our results should provide the appropriate theoretical background against which possible signals of new physics are searched for in these decays. Motivated by the experimental searches, we analyze also the Cabibbo allowed decays ( $D^0 \rightarrow K^{*0}l^+l^-$  and  $D_s^+ \rightarrow \rho^+l^+l^-$ ), which are the best candidates for their early detection, and the doubly Cabibbo suppressed decays ( $D^+ \rightarrow K^{*+}l^+l^-$  and  $D^0 \rightarrow K^{*0}l^+l^-$ ). Here the signals from new physics are not expected from the theoretical models usually considered.

On the experimental side, so far there are only upper bounds on the branching ratios of  $D \rightarrow Vl^+l^-$  decays from E653 and CLEO [13, 14], in the range  $10^{-3} - 10^{-4}$ , but these are expected to improve in the future.

In Sec. II we present the details of our approach and we define the approximations used. In Sec. III we give the results of our calculations and we summarize in Sec. IV.

## II. MODEL DESCRIPTION

### A. Long distance contributions

In this subsection we present the general framework used for calculating the long distance amplitudes, while the details of the model employed are given in subsection II C. The long distance contribution in  $D \rightarrow Vl^+l^-$  decays is due to the effective nonleptonic weak Lagrangian, which induces the weak transition between the initial and final hadronic state. The weak transition has to be accompanied by the emission of a virtual photon, which finally decays into a lepton antilepton pair. The effective nonleptonic weak Lagrangian responsible for charm meson decays is

$$\mathcal{L}_{LD} = -\frac{G_F}{\sqrt{2}} V_{uq_i} V_{cq_j}^* [a_1 (\bar{u}q_i)^\mu (\bar{q}_j c)_\mu + a_2 (\bar{u}c)_\mu (\bar{q}_j q_i)^\mu], \quad (1)$$

where  $(\bar{\psi}_1 \psi_2)^\mu \equiv \bar{\psi}_1 \gamma^\mu (1 - \gamma^5) \psi_2$ ,  $q_{i,j}$  represent the fields of  $d$  or  $s$  quarks,  $V_{ij}$  are the CKM matrix elements and  $G_F$  is the Fermi constant. In our calculation we use  $a_1 = 1.26$  and  $a_2 = -0.55$  as found in [15], from an extensive application of (1) to the study of nonleptonic  $D$  decays.

The virtual photon emission from the hadronic states is taken in our approach to proceed through two different mechanisms:

- (i) In the *nonresonant mechanism* the photon is emitted directly from the initial  $D$  state.
- (ii) In the *resonant mechanism*, apart from the final vector meson  $V$ , an additional neutral vector meson  $V_0$  is produced, which converts to a photon through vector meson dominance (VMD). In this case, a nonleptonic weak decay  $D \rightarrow VV_0$  is followed by the transition  $V_0 \rightarrow \gamma^* \rightarrow l^+l^-$ , where  $V_0$  is a short-lived vector meson  $\rho^0$ ,  $\omega$  or  $\phi$ .

The evaluation of the matrix elements of the product of two currents (1) requires nonperturbative techniques and we are forced to use some approximation. We have undertaken to use systematically the factorization approximation, where the matrix element of the product of two currents is approximated by

$$\langle V \gamma | (\bar{q}_i q_j)^\mu (\bar{q}_k c)_\mu | D \rangle = \langle V | (\bar{q}_i q_j)^\mu | 0 \rangle \langle \gamma | (\bar{q}_k c)_\mu | D \rangle$$

$$\begin{aligned}
& + \langle \gamma | (\bar{q}_i q_j)^\mu | 0 \rangle \langle V | (\bar{q}_k c)_\mu | D \rangle \\
& + \langle V \gamma | (\bar{q}_i q_j)^\mu | 0 \rangle \langle 0 | (\bar{q}_k c)_\mu | D \rangle .
\end{aligned} \tag{2}$$

The first two terms are the spectator contributions, in the following denoted by  $A_{Spec,\gamma}$  and  $A_{Spec,V}$ , respectively, and the third term is the weak annihilation contribution, denoted by  $A_{Annih}$ . Here  $\gamma$  denotes the virtual photon.

To calculate the matrix elements in (2) we use the hybrid model, which combines heavy quark effective theory (HQET) and chiral Lagrangian [16]-[18], which has been successfully employed already for  $D$  meson decays in several papers [16]-[26]. A very detailed description of the hybrid model and its previous applications is given in [18].

The relevant hadronic degrees of freedom for the present calculation are heavy pseudoscalar ( $D$ ) and vector mesons ( $D^*$ ) and light pseudoscalar ( $P$ ) and vector ( $V$ ) mesons. Within this approach the diagrams that contribute to the amplitudes  $A_{Spec,\gamma}$ ,  $A_{Spec,V}$  and  $A_{Annih}$  (2) are shown in Figs. 1a, 1b and 1c, respectively. Different diagrams in Fig. 1 are denoted by the roman numbers from  $I - VIII$ . The diagrams  $III$  and  $IV$  represent nonresonant contribution (mechanism (i)). All the remaining diagrams, which proceed through the intermediate short-lived vector meson  $V_0$  ( $\rho$ ,  $\omega$  and  $\phi$ ), represent the *resonant contribution* (mechanism (ii)). The resonant amplitude is represented in the whole  $q^2$  region by the Breit-Wigner vector meson propagator. ( $q$  is the sum of lepton and antilepton momenta). In the regions of  $q^2$  far away from  $m_{V_0}^2$ , the resonant amplitude is given therefore solely by the tail of the Breit-Wigner vector meson propagator. The square in each diagram of Fig. 1 denotes the weak transition due to the effective Lagrangian  $\mathcal{L}_{LD}$  (1). This Lagrangian contains a product of two left handed quark currents  $(\bar{q}_k q_l)^\mu$ , each denoted by a dot on Fig. 1. The left handed currents will be expressed in terms of the relevant hadronic degrees of freedom:  $D$ ,  $D^*$ ,  $P$  and  $V$ . In our notation the hadronic current  $J_2$  in the diagram  $III$ , for example, creates  $V$  meson, while the hadronic current  $J_1$  annihilates  $D$  and creates  $V_0$  at the same time.

In the model we use, there is no contribution of  $J/\Psi$  or other  $\bar{c}c$  excited states. The contribution that would arise by the exchange of this mesons is effectively described by the diagram  $III$  of Fig. 1, where  $\bar{c}c$  exchange is “hidden” in the  $DD^*\gamma$  coupling. The alternative approach of a direct  $\bar{c}c$  exchange would require the knowledge of their couplings to photons over a wide region of  $q^2$ , of which one has only rudimentary knowledge [27].

## B. Short distance contributions due to $c \rightarrow ul^+l^-$

In addition to long distance dynamics, the Cabibbo suppressed decays  $D^0 \rightarrow \rho^0 l^+ l^-$ ,  $D^0 \rightarrow \omega l^+ l^-$ ,  $D^0 \rightarrow \phi l^+ l^-$ ,  $D^+ \rightarrow \rho^+ l^+ l^-$  and  $D_s^+ \rightarrow K^{*+} l^+ l^-$  can

also be driven by the short distance  $c \rightarrow ul^+l^-$  transition. The short distance part in  $D \rightarrow Vl^+l^-$  decays will turn out in general to be much smaller than the long distance part. However, we shall find that in the case of  $D^0 \rightarrow \rho^0(\omega)l^+l^-$  the short distance part is of the same order of magnitude as the nonresonant part of the long distance contribution. In this subsection we estimate the size of the short distance amplitudes, which is *nonresonant* in its nature.

The effective Lagrangian for FCNC transition  $c \rightarrow ul^+l^-$  arises from  $WW$  exchange box diagrams and  $Z$  and  $\gamma^*$  penguin operators [4]. It has been obtained using the similar results for  $s \rightarrow dl^+l^-$  decay [28]

$$\begin{aligned} \mathcal{L}_{SD} &= \frac{G_F}{\sqrt{2}} \frac{e^2}{16\pi^2 \sin^2\theta_W} \\ &\times \sum_{i=d,s,b} V_i \left[ \bar{u}\gamma_\mu(1-\gamma_5)c \left( A_i \bar{l}\gamma^\mu(1-\gamma_5)l + B_i \bar{l}\gamma^\mu(1+\gamma_5)l \right) \right. \\ &\quad \left. - 2im_c \sin^2\theta_W F_2^i q^\nu \bar{u}\sigma_{\mu\nu}(1+\gamma_5)c \bar{l}\gamma^\mu(1-\gamma_5)l \right], \end{aligned} \quad (3)$$

where the Willson coefficients  $A_i$ ,  $B_i$  and  $F_2^i$  are given in Appendix A and  $V_i$  are the CKM coefficients,  $V_i = V_{ci}^*V_{ui}$ . The expression (3) does not contain the QCD corrections, which have not been studied for  $c \rightarrow ul^+l^-$  decays so far. When referring to these corrections for  $c \rightarrow ul^+l^-$ , one is reminded that in the case of  $c \rightarrow u\gamma$  decay there is a huge QCD enhancement [8, 11], which is due to the following reason: The effect of QCD is that the Wilson coefficient  $c_7(m_c)$ , responsible for the magnetic penguin decay  $c \rightarrow u\gamma$ , obtains the admixture of the other Wilson coefficients evaluated at the scale  $m_W$  in the leading order  $c_i(m_W)$ ,  $i = 1..10$ . Since  $c_7(m_W)$  is extremely suppressed compared to some other Wilson coefficients  $c_i(m_W)$ , the resulting  $c_7(m_c)$  is much bigger than  $c_7(m_W)$  and a huge QCD enhancement for  $c \rightarrow u\gamma$  occurs. In the  $c \rightarrow ul^+l^-$  decay on the other hand, the responsible Wilson coefficients  $A(m_W)$  and  $B(m_W)$ , which do not contribute for the real photons, are not suppressed in the lowest order and one would not expect large QCD effects on them as one has learned from estimation of  $s \rightarrow dl^+l^-$  [29]. The coefficient of the magnetic transition  $F_2(m_W)$ , which is proportional to Wilson coefficient  $c_7(m_W)$ , indeed acquires large QCD correction, however it is strongly suppressed in the lowest order. Since we are only interested in the rough estimation of the short distance contribution in  $D \rightarrow Vl^+l^-$  and the last term in (3) is much less important than the other two for such decays [29], we neglect the last term altogether, using the approximation explained in Appendix A.

The Lagrangian  $\mathcal{L}_{SD}$  (3) then gives the branching ratio for inclusive  $c \rightarrow ul^+l^-$  process

$$\frac{\Gamma(c \rightarrow ul^+l^-)}{\Gamma(D^0)} = \frac{G_F^2 m_c^5}{192\pi^3 \Gamma(D^0)} \left( \frac{\alpha}{4\pi \sin^2\theta_W} \right)^2 [|V_i A_i|^2 + |V_i B_i|^2] = 2.9 \cdot 10^{-9} .$$

To predict the exclusive amplitudes for  $D \rightarrow Vl^+l^-$  induced by  $\mathcal{L}_{SD}$  (3), we have to evaluate the matrix elements

$$\langle V|\bar{u}\gamma_\mu(1-\gamma_5)c|D\rangle. \quad (4)$$

We shall do this by again using the hybrid model, which is described in the next subsection. The corresponding Feynman diagrams within this approach are given in Fig. 2. The squares in the diagrams denote the weak transition due to the short distance Lagrangian  $\mathcal{L}_{SD}$  (3). This Lagrangian contains a product of a quark and lepton weak currents, each denoted by a dot in Fig. 2. We remark, that these diagrams have a long distance counterpart, given by diagrams  $V$  and  $VI$  of Fig. 1, which represent the long distance  $c \rightarrow u\gamma$  transition [9, 29]

### C. Theoretical framework: chiral Lagrangians, heavy quark limit and vector meson dominance

Here we present the model, which we use to evaluate the matrix elements (2) and (4) needed to predict  $D \rightarrow Vl^+l^-$  amplitudes. The framework we use for our treatment is that of an effective Lagrangian, which embodies two important approximate symmetries of QCD, the infinite heavy quark  $Q$  mass limit ( $m_Q \rightarrow \infty$ ) and the chiral limit for light quarks, namely  $(m_u, m_d, m_s) \rightarrow 0$ . This approach, which was developed during the last few years ([16]-[26] and additional references quoted in [18]), has been used with a good measure of success to treat strong, electromagnetic and weak decays of  $D$  and  $B$  mesons. Obviously, an effective Lagrangian approach has also its weakness, as it involves a number of unknown coupling constants. Fortunately, the use of observed processes makes it possible to determine a good proportion of them, as detailed in this and the next subsection. Moreover, the use of form factors alleviates the limitations on the range in which the basic assumptions of the model hold to a good accuracy. The model and its various applications till now are well exposed in a recent review [18]. In the present subsection, we describe those parts which are needed for our calculation. We introduce now the strong and electromagnetic interaction Lagrangians for the heavy (hadrons containing  $c$  quark) and light (hadrons containing only light  $u$ ,  $d$  and  $s$  quarks) sector and the relevant weak currents. At the end of the section we discuss the values of free parameters, that enter the Lagrangians and currents in our model. Our strong and electromagnetic Lagrangian [16]-[18] is invariant under heavy quark spin ( $SU(2)$ ), chiral ( $SU(3)_L \times SU(3)_R$ ), Lorentz, parity and  $U(1)$  gauge transformation [18]. The light vector mesons are incorporated using the hidden symmetry approach [18, 30]. We are aware that using HQET, which converges very slowly in the case of  $c$  quark, presents a rather rough approximation. In spite of that,

the HQET approach, which helps to reduce the number of free parameters, has been successfully applied in many  $D$  decays (e.g. [18] and references therein).

The light degrees of freedom are described by the  $3 \times 3$  Hermitian matrices

$$\Pi = \begin{pmatrix} \frac{\pi^0}{\sqrt{2}} + \frac{\eta_8}{\sqrt{6}} + \frac{\eta_0}{\sqrt{3}} & \pi^+ & K^+ \\ \pi^- & \frac{-\pi^0}{\sqrt{2}} + \frac{\eta_8}{\sqrt{6}} + \frac{\eta_0}{\sqrt{3}} & K^0 \\ K^- & \bar{K}^0 & -\frac{2\eta_8}{\sqrt{6}} + \frac{\eta_0}{\sqrt{3}} \end{pmatrix} \quad (5)$$

and

$$\rho_\mu = \begin{pmatrix} \frac{\rho_\mu^0 + \omega_\mu}{\sqrt{2}} & \rho_\mu^+ & K_\mu^{*+} \\ \rho_\mu^- & \frac{-\rho_\mu^0 + \omega_\mu}{\sqrt{2}} & K_\mu^{*0} \\ K_\mu^{*-} & \bar{K}_\mu^{*0} & \phi_\mu \end{pmatrix}, \quad F_{\mu\nu}(\rho) = \partial_\mu \rho_\nu - \partial_\nu \rho_\mu + [\rho_\mu, \rho_\nu] \quad (6)$$

for the pseudoscalar and vector mesons, respectively. They are usually expressed through the combinations

$$u = \exp\left(\frac{i\Pi}{f}\right), \quad (7)$$

where  $f \simeq f_\pi = 132$  MeV is the pion pseudoscalar decay constant and

$$\hat{\rho}_\mu = i \frac{\tilde{g}_V}{\sqrt{2}} \rho_\mu, \quad (8)$$

where  $\tilde{g}_V$  is fixed in the case of the exact flavor symmetry to be the  $VPP$  coupling  $\tilde{g}_V = 5.9$  [30].

The most general strong Lagrangian for the light mesons in the leading order of chiral perturbation theory is [30]

$$\mathcal{L}_{light}^1 = -\frac{f^2}{2} \{tr(\mathcal{A}_\mu \mathcal{A}^\mu) + a tr[(\mathcal{V}_\mu - \hat{\rho}_\mu)^2]\} + \frac{1}{2\tilde{g}_V^2} tr[F_{\mu\nu}(\hat{\rho}) F^{\mu\nu}(\hat{\rho})], \quad (9)$$

where we have introduced two currents

$$\mathcal{V}_\mu = \frac{1}{2}(u^\dagger D_\mu u + u D_\mu u^\dagger) \quad \text{and} \quad \mathcal{A}_\mu = \frac{1}{2}(u^\dagger D_\mu u - u D_\mu u^\dagger). \quad (10)$$

Demanding the Lagrangian (9) to be invariant under the local gauge transformation, corresponding to the electro-magnetic  $U(1)$  transformation in QCD, we define the covariant derivatives as

$$D_\mu u = (\partial_\mu + \hat{B}_\mu)u \quad \text{and} \quad D_\mu u^\dagger = (\partial_\mu + \hat{B}_\mu)u^\dagger,$$

with  $\hat{B}_\mu = ieB_\mu Q$ ,  $Q = \text{diag}(2/3, -1/3, -1/3)$  and  $B_\mu$  being the photon field. The constant  $a$  (9) is in principle a free parameter. We fix it to  $a = 2$  [30] assuming the exact vector meson dominance, where the pseudoscalars interact

with the photon only through vector mesons. With this choice, the photon - vector meson interaction given by the second term of Lagrangian (9) is

$$\mathcal{L}_{V\gamma} = -e\tilde{g}_V f^2 B_\mu (\rho^{0\mu} + \frac{1}{3}\omega^\mu - \frac{\sqrt{2}}{3}\phi^\mu) . \quad (11)$$

Instead of using the exact  $SU(3)$  symmetry values  $\tilde{g}_V = 5.9$  and  $f = 132 \text{ MeV}$ , we express the  $V\gamma$  couplings in terms of the measurable quantities  $g_\rho$ ,  $g_\omega$  and  $g_\phi$  defined by the matrix element of the corresponding vector current  $J_V^\mu$

$$\langle V(\epsilon_V, q) | J_V^\mu | 0 \rangle = g_V(q^2) \epsilon^{*\mu}(q) . \quad (12)$$

In our calculation we use the values  $g_V$  given in Table 2, which have been directly measured in the leptonic  $V \rightarrow l^+ l^-$  decays, and we make the assumption  $g_V(q^2) = g_V(m_V^2) \equiv g_V$ . The photon - vector meson interaction Lagrangian (11) defined through the constants  $g_V$  is

$$\mathcal{L}_{V\gamma} = -\frac{e}{\sqrt{2}} (g_\rho \rho^{0\mu} + \frac{g_\omega}{3} \omega^\mu - \frac{\sqrt{2}g_\phi}{3} \phi^\mu) B_\mu . \quad (13)$$

As far as the calculation of the amplitudes for the diagrams of Fig. 1 is concerned, the Lagrangian  $\mathcal{L}_{light}$  (9) provides also the  $VVV$  vertex given by the third term in (9). The  $VVV$  vertex is present in the diagram *VIII* of Fig. 1, which describes the photon emission from the charged vector meson.

We need also the  $PV\gamma$  vertex, which is present in the diagram *VII* of Fig. 1. This interaction term can be generated only in the next-to-leading order of chiral perturbation theory as [18]

$$\mathcal{L}_{light}^2 = -4 \frac{C_{VV\Pi}}{f} \epsilon^{\mu\nu\alpha\beta} Tr(\partial_\mu \rho_\nu \partial_\alpha \rho_\beta \Pi) , \quad (14)$$

where  $C_{VV\Pi}$  is free parameter.

Both the heavy pseudoscalar and the heavy vector mesons are incorporated in a  $4 \times 4$  matrix

$$H_a = \frac{1+\not{v}}{2} (P_{a\mu}^* \gamma^\mu - P_a \gamma_5) , \quad \bar{H}_a = \gamma^0 H_a^\dagger \gamma^0 = (P_{a\mu}^{*\dagger} \gamma^\mu + P_a^\dagger \gamma_5) \frac{1+\not{v}}{2} , \quad (15)$$

where  $a = 1, 2, 3$  is the  $SU(3)_V$  index of the light flavors and  $P_{a\mu}^*$ ,  $P_a$  annihilate a spin 1 and spin 0 heavy meson  $Q\bar{q}_a$  of velocity  $v$ , respectively. The strong and electromagnetic Lagrangian in the heavy sector have to provide us with the  $DD\gamma$ ,  $DD^*\gamma$  and  $DD^*V$  vertices. The first vertex describes the photon emission from the charged  $D$  meson and is generated in the leading order of HQET (invariant under heavy quark symmetry and  $U(1)$  gauge transformation with minimal number of derivatives) as [17, 18]

$$\mathcal{L}_{heavy}^1 = iTr[H_a v^\mu (\partial_\mu + \mathcal{V}_\mu - \frac{2}{3}ieB_\mu) \bar{H}_a] \quad (16)$$



The  $DD^*\gamma$  and  $DD^*V$  vertices can be generated only in the next-to-leading order of the heavy quark and chiral expansion and are described by [17, 18]

$$\mathcal{L}_{heavy}^2 = -\lambda' Tr[H_a \sigma_{\mu\nu} F^{\mu\nu}(B) \bar{H}_a] + i\lambda Tr[H_a \sigma_{\mu\nu} F^{\mu\nu}(\hat{\rho})_{ab} \bar{H}_b]. \quad (17)$$

The first term contributes to the diagram *III* Fig. 1, while the second term contributes to the diagrams *I* and *V* of Fig. 1 and the diagram *I* of Fig. 2. The  $\lambda$  and  $\lambda'$  are free parameters.

In addition to the strong and electromagnetic interaction, we have to specify the weak one. The effective weak Lagrangian responsible for the long distance contribution is given by  $\mathcal{L}_{LD}$  (1) and for the short distance contribution by  $\mathcal{L}_{SD}$  (3). As we deal with the probabilities for the weak decays of hadrons, we rewrite the quark weak currents in  $\mathcal{L}_{LD}$  (1) and  $\mathcal{L}_{SD}$  (3) in terms of hadronic degrees of freedom. The weak current  $\bar{q}_a \gamma^\mu (1 - \gamma^5) c$  containing a  $c$  quark and one light anti-quark  $\bar{q}_a$  transforms under chiral  $SU(3)_L \times SU(3)_R$  transformation as  $(\bar{3}_L, 1_R)$ . At the hadronic level we impose the same chiral transformation and we require the current to be linear in the heavy meson fields  $D^a$  and  $D_\mu^{*a}$  [16, 26]

$$\begin{aligned} J_a^\mu &= \frac{1}{2} i\alpha Tr[\gamma^\mu (1 - \gamma_5) H_b u_{ba}^\dagger] \\ &+ \alpha_1 Tr[\gamma_5 H_b (\hat{\rho}^\mu - \mathcal{V}^\mu)_{bc} u_{ca}^\dagger] + \alpha_2 Tr[\gamma^\mu \gamma_5 H_b v_\alpha (\hat{\rho}^\alpha - \mathcal{V}^\alpha)_{bc} u_{ca}^\dagger] + \dots \end{aligned} \quad (18)$$

The current (18) is the most general one in the leading  $1/m_c$  order of HQET and next to leading order of chiral perturbation theory. The first term is connected to the definition of the heavy meson decay constant  $\langle D(p) | (\bar{q}_a c)^\mu | 0 \rangle = -i f_D p^\mu$ , where  $\alpha = f_D \sqrt{m_D}$ . The second and third term contribute to the diagrams *II* and *VI* of Fig. 1 and diagram *II* of Fig. 2, where  $J_a^\mu$  (18) annihilates  $D$  meson and creates  $V$  or  $V_0$  meson at the same time. The constants  $\alpha_1$  and  $\alpha_2$  are free parameters.

#### D. The choice of the parameters

We now turn to the values of the coupling constants  $C_{VV\Pi}$ ,  $\lambda$ ,  $\lambda'$ ,  $\alpha_1$  and  $\alpha_2$ , which we need in the evaluation of the amplitudes of diagrams on Figs. 1 and 2.

The coupling  $C_{VV\Pi}$  can be determined in the case of the exact  $SU(3)$  flavor symmetry following the hidden symmetry approach of [30] and is found to be  $|C_{VV\Pi}| = 3\tilde{g}_V^2/32\pi^2 = 0.33$ . Experimentally, it can be directly determined from the  $V \rightarrow PV_0 \rightarrow P\gamma$  decay rates. In the following we will use the average value of  $C_{VV\Pi}$ , obtained from the measurements of different  $V \rightarrow PV_0 \rightarrow P\gamma$  decays  $|C_{VV\Pi}| = 0.31$  [9], which is close to its  $SU(3)$  limit.

We determine the three parameters  $\lambda$ ,  $\alpha_1$  and  $\alpha_2$  using three values related to the helicity amplitudes  $Br = 0.048 \pm 0.004$ ,  $\Gamma_L/\Gamma_T = 1.23 \pm 0.13$  and  $\Gamma_+/\Gamma_- = 0.16 \pm 0.04$  for the process  $D^+ \rightarrow \bar{K}^{*0} l^+ \nu_l$  [16], taken from the average of data from different experiments [14]. We get four sets of solutions for  $\lambda$ ,  $\alpha_1$  and  $\alpha_2$  [16] and we choose the set, which gives the best fit with a number of the nonleptonic decays  $D \rightarrow PV$ ,  $D \rightarrow VV$  and  $D \rightarrow PP$  [20]:

$$\lambda = -0.34 \pm 0.07, \quad \alpha_1 = -0.14 \pm 0.01, \quad \text{and} \quad \alpha_2 = -0.83 \pm 0.4.$$

In order to gain information on  $\lambda'$  we turn to an analysis of  $D^{*0} \rightarrow D^0 \gamma$ ,  $D^{*+} \rightarrow D^+ \gamma$  and  $D_s^{*+} \rightarrow D_s^+ \gamma$  decays. Experimentally, only the ratios  $R_\gamma^0 = \Gamma(D^{*0} \rightarrow D^0 \gamma)/\Gamma(D^{*0} \rightarrow D^0 \pi^0)$  and  $R_\gamma^+ = \Gamma(D^{*+} \rightarrow D^+ \gamma)/\Gamma(D^{*+} \rightarrow D^+ \pi^0)$  are known [14]. Taking the  $R_\gamma^0 = 0.616$  and  $R_\gamma^+ = 0.036$  [14], we obtain two sets of solutions for  $|\lambda'/g|$  and  $|\lambda/g|$ , which gives two solutions for  $|\lambda'/\lambda|$ . The first is  $|\lambda'/\lambda| = 0.77$  and the second is  $|\lambda'/\lambda| = 0.21$  [9]. Taking  $\lambda = -0.34$  we get four possibilities for  $\lambda' = \pm 0.26, \pm 0.071$ , which all have to be considered.

### III. THE AMPLITUDES AND BRANCHING RATIOS FOR NINE $D \rightarrow Vl^+l^-$ DECAYS

#### A. The amplitudes

In this section we turn to the amplitudes and branching ratios for the nine  $D \rightarrow Vl^+l^-$  decays. The interaction Lagrangians (9), (13), (14), (16), (17) and the weak currents (12), (18) provide us with the vertices in the kinematical region, where the heavy quark and chiral symmetry are good (i.e. the velocity of the heavy mesons changes only slightly in the interaction and the energy of the light mesons is small). The problem is how to extrapolate the amplitudes to the rest of the kinematical region allowed in  $D \rightarrow Vl^+l^-$  decays. We assume, that the vertices do not change significantly throughout the kinematical region, which is a reasonable assumption in  $D$  decays. At the same time we use the full heavy meson propagators  $1/(p^2 - m^2)$  instead of the HQET propagators  $1/(2mv \cdot k)$ . We account for the short life time of the intermediate neutral vector meson  $V_0$  by using the Breit Wigner form for the  $V_0$  propagator

$$-i \frac{g_{\mu\nu} - \frac{q_\mu q_\nu}{m_{V_0}^2}}{q^2 - m_{V_0}^2 + i\Gamma_{V_0} m_{V_0}},$$

where  $\Gamma_{V_0}$  is the decay width of the  $V_0$  meson and  $q$  is its momentum. Then, using the interaction Lagrangians (1), (3), (9), (13), (14), (16), (17) and the weak currents (12), (18), the calculation of the amplitudes for long distance diagrams on Fig. 1 and short distance diagrams on Fig. 2 is straightforward. The calculated amplitudes for different diagrams have in general different Lorentz structure. It is convenient to treat the amplitudes of similar Lorentz structure

together. Then, the sum of the amplitudes within the model described above is given by the expression

$$\begin{aligned} \mathcal{A} [D(p) \rightarrow V(\epsilon_{(V)}, p_{(V)}) l^+(p_+) l^-(p_-)] &= -\frac{G_F}{\sqrt{2}} e^2 f_{Cab} \frac{1}{q^2} \\ &\times \epsilon_{(V)\beta} \bar{u}(p_-) \gamma_\nu v(p_+) [\epsilon^{\mu\nu\alpha\beta} q_\mu p_\alpha A_{PC} + iA_{PV}^{\beta\nu}], \end{aligned} \quad (19)$$

where  $q = p_- + p_+$  is the momentum of the intermediate virtual photon and the corresponding Cabibbo factors  $f_{Cab}$  are given in Table 1.  $A_{PC}$  and  $A_{PV}^{\beta\nu}$  correspond to parity conserving and parity violating amplitudes, respectively. They get contributions from different diagrams in Fig. 1 (long distance) and Fig. 2 (short distance). The short distance amplitudes  $A_{PC}$  and  $A_{PV}^{\beta\nu}$  for the Cabibbo suppressed decays are given in Appendix A. The long distance amplitudes  $A_{PC}$  and  $A_{PV}^{\beta\nu}$  for the Cabibbo allowed, suppressed and doubly suppressed decays are given in Appendix B.

The decay width for  $D \rightarrow Vl^+l^-$  is given by the square of the amplitude, summed over the polarizations of the three particles in the final state and integrated over the three body phase space

$$\Gamma = \frac{1}{2m_D(2\pi)^5} \sum_{polar.} \int |\mathcal{A}(p_{(V)}, p_+, p_-)|^2 \frac{d^3p_{(V)}}{2p_{(V)}^0} \frac{d^3p_+}{2p_+^0} \frac{d^3p_-}{2p_-^0} \delta(p_{(V)} + p_+ + p_- - p). \quad (20)$$

## B. Discussion of the results

Firstly, we present the results for the decays with the muon final state  $D \rightarrow V\mu^+\mu^-$  and we comment on the decays  $D \rightarrow Ve^+e^-$  in the end. The branching ratios for the Cabibbo allowed, suppressed and doubly suppressed  $D \rightarrow V\mu^+\mu^-$  decays are presented in Table 1. The last column presents the experimental upper bounds [13, 14]. The other columns present our theoretical predictions, where the error bars are due to the uncertainty of the model parameters  $\lambda'$  and  $C_{VV\Pi}$ , which can have any of the values  $\lambda' = \pm 0.07, \pm 0.26$  and  $C_{VV\Pi} = \pm 0.31$ . The total branching ratio  $Br(total)$  containing long (Fig. 1) and short distance (Fig. 2) contributions is given in the fifth column. The third column presents the short distance part of the branching ratio  $Br(SD)$  calculated from (3), which is present only in the Cabibbo suppressed decays. The fourth column presents only the nonresonant part of the long distance contribution  $Br(LD_{nonr})$ . This part is bigger for the charged  $D$  meson decays, where it is mainly due to the diagram *IV* of Fig. 1. For the neutral  $D$  meson decays, the diagram *IV* vanishes and the remaining nonresonant diagram *III* has smaller amplitude, which is proportional to  $\lambda'$ . The parameter  $\lambda' = \pm 0.07, \pm 0.26$  has large uncertainty and we are only able to quote the upper limit for  $Br(LD_{nonr})$ .

Apart from the Cabibbo structure, the branching ratios depend mainly on whether the initial (and final) state is charged or neutral, with bigger branching ratio in the former case. We present also the distributions  $(1/\Gamma_D)d\Gamma(D \rightarrow V\mu^+\mu^-)/dq^2$  as a function of  $q^2$  ( $q^2$  is invariant  $\mu^+\mu^-$  mass) for the typical representatives of the Cabibbo allowed ( $D_s^+ \rightarrow \rho^+\mu^+\mu^-$  in Fig. 3 and  $D^0 \rightarrow \bar{K}^{*0}\mu^+\mu^-$  in Fig. 4) and suppressed ( $D^0 \rightarrow \rho^0\mu^+\mu^-$  in Fig. 5 and  $D_s^+ \rightarrow K^{*+}\mu^+\mu^-$  in Fig. 6), neutral or charged  $D$  meson decays. The short distance contribution (dot-dashed line) due to  $c \rightarrow ul^+l^-$  transition is present only in the Cabibbo suppressed decays and it turns out to be much smaller than the long distance contribution. Concerning the long distance contribution, the resonant part is bigger than the nonresonant part (dashed line), except perhaps in the case of charged  $D$  meson decays at the low  $q^2$  (see Figs. 3-6). Note, that the nonresonant LD contribution is generally smaller than the resonant LD contributions even in the regions well outside the resonance peak at  $q^2 = m_{V_0}^2$ . It is interesting to remark, that the short distance and nonresonant long distance contributions are comparable for Cabibbo suppressed neutral  $D$  meson decays  $D^0 \rightarrow \rho^0l^+l^-$  and  $D^0 \rightarrow \omega l^+l^-$ .

In the decays with the electron final state  $D \rightarrow Ve^+e^-$  the lowest kinematically allowed  $q^2$  is  $q_{min}^2 = (2m_e)^2$ , which is smaller than  $q_{min}^2 = (2m_\mu)^2$  in the  $D \rightarrow V\mu^+\mu^-$  case. In the region  $q^2 > (2m_\mu)^2$  the electron rates are practically equal to the muon rates. In the region  $q^2 < (2m_\mu)^2$ , however, the rates for  $D \rightarrow Ve^+e^-$  are extremely enhanced due to the photon propagator  $1/q^2$ . However, the region down to  $q_{min}^2 = (2m_e)^2$  requires a more accurate treatment of the  $q^2$  dependence when  $q^2$  approaches to 0, which is beyond our scope here. We have calculated the  $D \rightarrow Ve^+e^-$  branching ratios with the lower cut off  $q^2 = (2m_\mu)^2$  and have obtained values which are very close to the  $D \rightarrow V\mu^+\mu^-$  branching ratios (the  $D \rightarrow V\mu^+\mu^-$  branching ratios are obtained integrating over the whole  $q^2 = [(2m_\mu)^2, (m_D - m_V)^2]$  region).

The Cabibbo allowed decays  $D^0 \rightarrow \bar{K}^{*0}\mu^+\mu^-$  and  $D_s^+ \rightarrow \rho^+\mu^+\mu^-$  with the predicted branching ratios of the order  $10^{-6}$  and  $10^{-5}$ , respectively, have the best probability for their early detection. Note that their branching ratios are not far below the present experimental upper bound.

In the Cabibbo suppressed decays, the short distance contribution due to FCNC transition  $c \rightarrow ul^+l^-$  has branching ratio of order  $Br(SD) \sim 10^{-10}$  and is therefore well masked by the long distance branching ratios of order  $10^{-7}$ . Obviously, to observe the FCNC transition  $c \rightarrow u$  within the Standard Model, one must most likely look for other possibilities. Still, new physics could enhance the SD part to be of the same order as the LD part or bigger [2, 5, 6]. In this case the branching ratios well above  $10^{-7}$  for Cabibbo suppressed decays  $D \rightarrow V\mu^+\mu^-$  would signal new physics. As the present experimental upper

bound is much higher, these decays still contain a large discovery window.

#### IV. SUMMARY

We have calculated the long and short distance contributions for nine  $D \rightarrow Vl^+l^-$  decays within the Standard Model. The short distance contribution is present only in the Cabibbo suppressed decays and is due to the flavour changing neutral transition  $c \rightarrow ul^+l^-$ . The long distance contribution is composed of the resonant part, which arises from the intermediate light vector meson  $V_0$  exchange ( $D \rightarrow VV_0 \rightarrow V\gamma \rightarrow Vl^+l^-$ ), and the nonresonant part, which arises from the direct photon emission ( $D \rightarrow V\gamma \rightarrow Vl^+l^-$ ). The branching ratios are calculated using an effective Lagrangian, which combines heavy quark symmetry and chiral perturbation theory, and are given in Table 1. The most frequent decays are the Cabibbo allowed decays, which are expected at the rates, that are not much lower than the present experimental upper limit:  $D_s^+ \rightarrow \rho^+\mu^+\mu^-$  is expected at the branching ratio of approximately  $3 \cdot 10^{-5}$ , while  $D^0 \rightarrow \bar{K}^{*0}\mu^+\mu^-$  is expected at  $1.7 \cdot 10^{-6}$ . The Cabibbo suppressed decays on the other hand, are typically expected at  $[3 - 7] \cdot 10^{-7}$  range for  $D^0 \rightarrow \rho^0(\omega)\mu^+\mu^-$  and  $D_s^+ \rightarrow K^{*+}\mu^+\mu^-$  decays and in the  $10^{-6}$  range for  $D^+ \rightarrow \rho^+\mu^+\mu^-$  decay. Accordingly, branching ratios well above  $10^{-7}$  for Cabibbo suppressed decays could signal new physics. In all the Cabibbo suppressed decays the short distance contribution is well masked in the Standard Model by the resonant long distance contribution. In the case of  $D^0 \rightarrow \rho^0(\omega)l^+l^-$  decays, however, the short distance contribution is of comparable size as the nonresonant long distance part.

$D \rightarrow V\mu^+\mu^-$	$f_{Cab}$	$Br(SD)$	$Br(LD_{nonr})$	$Br(total)$	$Br(exp)$
$D^0 \rightarrow \overline{K}^{*0}\mu^+\mu^-$	$a_2c^2$	0	$\leq 1.9 \cdot 10^{-8}$	$[1.6 - 1.9] \cdot 10^{-6}$	$< 1.18 \cdot 10^{-3}$
$D_s^+ \rightarrow \rho^+\mu^+\mu^-$	$a_1c^2$	0	$4.0 \cdot 10^{-6}$	$[3.0 - 3.3] \cdot 10^{-5}$	
$D^0 \rightarrow \rho^0\mu^+\mu^-$	$-a_2sc$	$9.7 \cdot 10^{-10}$	$\leq 4.8 \cdot 10^{-10}$	$[3.5 - 4.7] \cdot 10^{-7}$	$< 2.3 \cdot 10^{-4}$
$D^0 \rightarrow \omega\mu^+\mu^-$	$-a_2sc$	$9.1 \cdot 10^{-10}$	$\leq 3.7 \cdot 10^{-10}$	$[3.3 - 4.5] \cdot 10^{-7}$	$< 8.3 \cdot 10^{-4}$
$D^0 \rightarrow \phi\mu^+\mu^-$	$a_2sc$	0	$\leq 1.1 \cdot 10^{-9}$	$[6.5 - 9.0] \cdot 10^{-8}$	$< 4.1 \cdot 10^{-4}$
$D^+ \rightarrow \rho^+\mu^+\mu^-$	$-a_1sc$	$4.8 \cdot 10^{-9}$	$2.7 \cdot 10^{-7}$	$[1.5 - 1.8] \cdot 10^{-6}$	$< 5.6 \cdot 10^{-4}$
$D_s^+ \rightarrow K^{*+}\mu^+\mu^-$	$a_1sc$	$1.6 \cdot 10^{-9}$	$1.5 \cdot 10^{-7}$	$[5.0 - 7.0] \cdot 10^{-7}$	$< 1.4 \cdot 10^{-3}$
$D^+ \rightarrow K^{*+}\mu^+\mu^-$	$-a_1s^2$	0	$1.0 \cdot 10^{-8}$	$[3.1 - 3.7] \cdot 10^{-8}$	$< 8.5 \cdot 10^{-4}$
$D^0 \rightarrow \overline{K}^{*0}\mu^+\mu^-$	$-a_2s^2$	0	$\leq 5.0 \cdot 10^{-11}$	$[4.4 - 5.1] \cdot 10^{-9}$	

Table 1: The branching ratios for the Cabibbo allowed, suppressed and doubly suppressed  $D \rightarrow V\mu^+\mu^-$  decays. The last column presents the experimental upper bounds [13, 14], while the other columns present our theoretical predictions. The total branching ratio  $Br(total)$  containing long (Fig. 1) and short distance (Fig. 2) contributions is given in the fifth column. The third column presents only the short distance part of the branching ratio  $Br(SD)$ . The fourth column presents only the nonresonant part of the long distance contribution  $Br(LD_{nonr})$ . The error bars in the Table are due to the uncertainty of the model parameters expressed by the possibilities  $\lambda' = \pm 0.07, \pm 0.26$  and  $C_{VV\Pi} = \pm 0.31$ . The branching ratios for  $D \rightarrow Ve^+e^-$  obtained with the lower cut off  $q^2 = (2m_\mu)^2$  ( $q^2$  the invariant  $\mu^+\mu^-$  mass) are almost exactly the same as the branching ratios for  $D \rightarrow V\mu^+\mu^-$  given in this Table. The second column gives the corresponding Cabibbo factors  $f_{Cab}$  in terms of the Cabibbo angle  $c = \cos \theta_C$  and  $s = \sin \theta_C$ .

## APPENDIX A: The short distance amplitudes

In this Appendix we list the values of the Willson coefficients  $A_i$ ,  $B_i$  and  $F_2^i$  in the short distance Lagrangian  $\mathcal{L}_{SD}$  (3) and give the resulting short distance amplitudes  $A_{PC}$  and  $A_{PV}^{\beta\nu}$  from (19).

The coefficients  $A_i$ ,  $B_i$  and  $F_2^i$  have been obtained in the leading order by Inami and Lim [28] and following the notation of [4] one has

$$\begin{aligned}
A_i &= C_i^{box} + C_i^Z - \sin^2 \theta_W (F_1^i + C_i^Z), \\
B_i &= -\sin^2 \theta_W (F_1^i + C_i^Z),
\end{aligned} \tag{21}$$

where  $C_i^{box}$ ,  $C_i^Z$ ,  $F_1^i$  and  $F_2^i$  are kinematic factors, which depend on the  $i$ th-quark mass through  $x_i = m_i^2/m_W^2$

$$\begin{aligned}
C_i^{box} &= \frac{3}{8} \left[ -\frac{1}{x_i - 1} + \frac{x_i \ln x_i}{(x_i - 1)^2} \right] - \gamma(\xi, x_i) \\
C_i^Z &= \frac{x_i}{4} - \frac{3}{8} \frac{1}{x_i - 1} + \frac{3}{8} \frac{2x_i^2 - x_i}{(x_i - 1)^2} \ln x_i + \gamma(\xi, x_i)
\end{aligned} \tag{22}$$

$$\begin{aligned}
F_1^i &= Q \left( \left[ \frac{1}{12} \frac{1}{x_i - 1} + \frac{13}{12} \frac{1}{(x_i - 1)^2} - \frac{1}{2} \frac{1}{(x_i - 1)^3} \right] x_i \right. \\
&+ \left. \left[ \frac{2}{3} \frac{1}{x_i - 1} + \left( \frac{2}{3} \frac{1}{(x_i - 1)^2} - \frac{5}{6} \frac{1}{(x_i - 1)^3} + \frac{1}{2} \frac{1}{(x_i - 1)^4} \right) x_i \right] \ln x_i \right) \\
&- \left[ \frac{7}{3} \frac{1}{x_i - 1} + \frac{13}{12} \frac{1}{(x_i - 1)^2} - \frac{1}{2} \frac{1}{(x_i - 1)^3} \right] x_i \\
&- \left[ \frac{1}{6} \frac{1}{x_i - 1} - \frac{35}{12} \frac{1}{(x_i - 1)^2} - \frac{5}{6} \frac{1}{(x_i - 1)^3} + \frac{1}{2} \frac{1}{(x_i - 1)^4} \right] x_i \ln x_i - 2\gamma(\xi, x_i) \\
F_2^i &= -Q \left( \left[ -\frac{1}{4} \frac{1}{x_i - 1} + \frac{3}{4} \frac{1}{(x_i - 1)^2} + \frac{3}{2} \frac{1}{(x_i - 1)^3} \right] x_i - \frac{3}{2} \frac{x_i^2 \ln x_i}{(x_i - 1)^4} \right) \\
&+ \left[ \frac{1}{2} \frac{1}{x_i - 1} + \frac{9}{4} \frac{1}{(x_i - 1)^2} + \frac{3}{2} \frac{1}{(x_i - 1)^3} \right] x_i - \frac{3}{2} \frac{x_i^3 \ln x_i}{(x_i - 1)^4} \quad (23)
\end{aligned}$$

The summation  $i$  in  $\mathcal{L}_{SD}$  (3) runs over down-like quarks ( $d$ ,  $s$  and  $b$ ) to which charm can couple, while  $Q = -1/3$  is the corresponding charge of the intermediate quarks (we note that  $F_1$  and  $F_2$  have been calculated in [4] using the wrong charge  $Q = 2/3$ ). The gauge dependent term  $\gamma(\xi, x_i)$  [28] cancels out in the combinations  $A_i$ ,  $B_i$  and  $F_2^i$  (21). Since the ratios  $x_d$ ,  $x_s$  and  $x_b$  are of orders  $10^{-8}$ ,  $10^{-6}$  and  $10^{-3}$  respectively, the terms proportional to the powers of  $x_i$  can be safely neglected in (22). With this approximation  $C_i^{box} = C_i^Z = -3/8$ ,  $F_1^i = -2 \ln x_i / (9x_i - 9)$  and  $F_2^i$  vanishes. In this limit the GIM cancelation occurs and we obtain

$$\sum V_i A_i = \sum V_i B_i \equiv A_{SD} = -0.065 \quad (24)$$

Consequently, the short distance Lagrangian (3) effectively contains only the vector lepton current  $\bar{l}\gamma^\mu l$  but not the axial vector  $\bar{l}\gamma^\mu \gamma_5 l$  one.

The short distance  $c \rightarrow ul^+l^-$  transition contributes only to the Cabibbo suppressed decays. Here we give the short distance contributions for the parity conserving  $A_{PC}$  and parity violating  $A_{PV}^{\beta\nu}$  amplitudes, which are needed to calculate the Cabibbo suppressed amplitudes  $\mathcal{A}[D(p) \rightarrow V(\epsilon_V, p_V) l^+(p_+) l^-(p_-)]$ , (19). Within the model used, these amplitudes are given by the diagrams on Fig. 2:

$$\begin{aligned}
A_{PC}(D^0 \rightarrow \rho^0 l^+ l^-) &= A_{PC}(D^0 \rightarrow \omega l^+ l^-) = A_{PC}(D^+ \rightarrow \rho^+ l^+ l^-) / \sqrt{2} \\
&= A_{PC}(D_s^+ \rightarrow K^{*+} l^+ l^-) / \sqrt{2} = 4 \frac{f_{D^*} \lambda \tilde{g}_V}{f_{Cab}} \sqrt{\frac{m_{D^*}}{m_D}} \frac{m_{D^*}}{q^2 - m_{D^*}^2} \frac{A_{SD} q^2}{16\pi^2 \sin^2 \theta_W}, \\
A_{PV}^{\beta\nu}(D^0 \rightarrow \rho^0 l^+ l^-) &= A_{PV}^{\beta\nu}(D^0 \rightarrow \omega l^+ l^-) = A_{PV}^{\beta\nu}(D^+ \rightarrow \rho^+ l^+ l^-) / \sqrt{2} \\
&= A_{PV}^{\beta\nu}(D_s^+ \rightarrow K^{*+} l^+ l^-) / \sqrt{2} = -2 \frac{\tilde{g}_V \sqrt{m_D}}{f_{Cab}} \left[ \alpha_1 g^{\beta\nu} - \alpha_2 \frac{q^\beta p^\nu}{m_D^2} \right] \frac{A_{SD} q^2}{16\pi^2 \sin^2 \theta_W}, \\
A_{PC}^{\beta\nu}(D^0 \rightarrow \phi^0 l^+ l^-) &= A_{PV}^{\beta\nu}(D^0 \rightarrow \phi l^+ l^-) = 0. \quad (25)
\end{aligned}$$

The last equation is a result of Eq. (4) and the quark content of the  $\phi$  meson. The relevant constants are presented in Appendix B.

## APPENDIX B: The long distance amplitudes

In this Appendix we give the expressions for the parity conserving  $A_{PC}$  and parity violating amplitudes  $A_{PV}^{\beta\nu}$ , which are needed to calculate the amplitudes  $\mathcal{A}[D(p) \rightarrow V(\epsilon_{(V)}, p_{(V)}) l^+(p_+) l^-(p_-)]$  (19) for nine  $D \rightarrow Vl^+l^-$  decays. The following amplitudes  $A_{PC}$  and  $A_{PV}^{\beta\nu}$  contain the long distance resonant and nonresonant contributions coming from the diagrams on Fig. 1. The coefficients and constants needed for the evaluation of the amplitudes will be given below:

$$\begin{aligned}
A_{PC}(D^0 \rightarrow \bar{K}^{*0}l^+l^-) &= 4J^{D^0} g_{K^*} f_{D^*} \sqrt{\frac{m_{D^*}}{m_D}} \frac{m_{D^*}}{m_{K^*}^2 - m_{D^*}^2} - 2K^{\bar{K}^{*0}} C_{VV\Pi} f_D m_D^2, \\
A_{PV}^{\beta\nu}(D^0 \rightarrow \bar{K}^{*0}l^+l^-) &= M^{D^0} g_{K^*} \sqrt{m_D} \left[ \alpha_1 g^{\beta\nu} - (\alpha_1 - \alpha_2) \frac{q \cdot p}{m_D^2} \frac{q^\beta q^\nu}{m_{V_0}^2} - \alpha_2 \frac{q^\beta p^\nu}{m_D^2} \right], \\
A_{PC}(D_s^+ \rightarrow \rho^+l^+l^-) &= 4J^{D_s^+} g_\rho f_{D_s^*} \sqrt{\frac{m_{D_s^*}}{m_{D_s}}} \frac{m_{D_s^*}}{m_\rho^2 - m_{D_s^*}^2} - 2K^{\rho^+} C_{VV\Pi} f_{D_s} m_{D_s}^2, \\
A_{PV}^{\beta\nu}(D_s^+ \rightarrow \rho^+l^+l^-) &= 2f_{D_s} g_\rho \left[ \frac{q^\beta p^\nu}{m_{D_s}^2 - m_\rho^2} - L^{\rho^+} \frac{g^{\beta\nu}}{2} (q^2 - m_\rho^2) \right] \\
&\quad + M^{D_s^+} g_\rho \sqrt{m_{D_s}} \left[ \alpha_1 g^{\beta\nu} - (\alpha_1 - \alpha_2) \frac{q \cdot p}{m_{D_s}^2} \frac{q^\beta q^\nu}{m_{V_0}^2} - \alpha_2 \frac{q^\beta p^\nu}{m_{D_s}^2} \right], \\
A_{PC}(D^0 \rightarrow \rho^0l^+l^-) &= -4 \frac{J^{D^0}}{\sqrt{2}} g_\rho f_{D^*} \sqrt{\frac{m_{D^*}}{m_D}} \frac{m_{D^*}}{m_\rho^2 - m_{D^*}^2} - 2K^{\rho^0} C_{VV\Pi} f_D m_D^2 \\
&\quad - N f_{D^*} \lambda \tilde{g}_V \frac{a_2 \sin \theta_C \cos \theta_C}{f_{Cab}} \sqrt{\frac{m_{D^*}}{m_D}} \frac{m_{D^*}}{q^2 - m_{D^*}^2}, \\
A_{PV}^{\beta\nu}(D^0 \rightarrow \rho^0l^+l^-) &= M^{D^0} g_\rho \sqrt{m_D} \left[ \alpha_1 g^{\beta\nu} - (\alpha_1 - \alpha_2) \frac{q \cdot p}{m_D^2} \frac{q^\beta q^\nu}{m_{V_0}^2} - \alpha_2 \frac{q^\beta p^\nu}{m_D^2} \right] \\
&\quad + \frac{N}{2} \tilde{g}_V \sqrt{m_D} \frac{a_2 \sin \theta_C \cos \theta_C}{f_{Cab}} \left[ \alpha_1 g^{\beta\nu} - \alpha_2 \frac{q^\beta p^\nu}{m_D^2} \right], \\
A_{PC}(D^0 \rightarrow \omega l^+l^-) &= 4 \frac{J^{D^0}}{\sqrt{2}} g_\omega f_{D^*} \sqrt{\frac{m_{D^*}}{m_D}} \frac{m_{D^*}}{m_\omega^2 - m_{D^*}^2} - 2K^\omega C_{VV\Pi} f_D m_D^2 \\
&\quad - N f_{D^*} \lambda \tilde{g}_V \frac{a_2 \sin \theta_C \cos \theta_C}{f_{Cab}} \sqrt{\frac{m_{D^*}}{m_D}} \frac{m_{D^*}}{q^2 - m_{D^*}^2}, \\
A_{PV}^{\beta\nu}(D^0 \rightarrow \omega l^+l^-) &= M^{D^0} g_\omega \sqrt{m_D} \left[ \alpha_1 g^{\beta\nu} - (\alpha_1 - \alpha_2) \frac{q \cdot p}{m_D^2} \frac{q^\beta q^\nu}{m_{V_0}^2} - \alpha_2 \frac{q^\beta p^\nu}{m_D^2} \right]
\end{aligned}$$



$$\begin{aligned}
& + \frac{N}{2} \tilde{g}_V \sqrt{m_D} \frac{a_2 \sin \theta_C \cos \theta_C}{f_{Cab}} \left[ \alpha_1 g^{\beta\nu} - \alpha_2 \frac{q^\beta p^\nu}{m_D^2} \right], \\
A_{PC}(D^0 \rightarrow \phi l^+ l^-) &= 4J^{D^0} g_\phi f_{D^*} \sqrt{\frac{m_{D^*}}{m_D} \frac{m_{D^*}}{m_\phi^2 - m_{D^*}^2}} - 2K^\phi C_{VV\Pi} f_D m_D^2, \\
A_{PV}^{\beta\nu}(D^0 \rightarrow \phi l^+ l^-) &= M^{D^0} g_\phi \sqrt{m_D} \left[ \alpha_1 g^{\beta\nu} - \left( \alpha_1 - \alpha_2 \frac{q \cdot p}{m_D^2} \right) \frac{q^\beta q^\nu}{m_{V_0}^2} - \alpha_2 \frac{q^\beta p^\nu}{m_D^2} \right], \\
A_{PC}(D^+ \rightarrow \rho^+ l^+ l^-) &= 4J^{D^+} g_\rho f_{D^*} \sqrt{\frac{m_{D^*}}{m_D} \frac{m_{D^*}}{m_\rho^2 - m_{D^*}^2}} - 2K^{\rho^+} C_{VV\Pi} f_D m_D^2 \\
& - \sqrt{2} N f_{D^*} \lambda \tilde{g}_V \frac{a_2 \sin \theta_C \cos \theta_C}{f_{Cab}} \sqrt{\frac{m_{D^*}}{m_D} \frac{m_{D^*}}{q^2 - m_{D^*}^2}}, \\
A_{PV}^{\beta\nu}(D^+ \rightarrow \rho^+ l^+ l^-) &= 2f_D g_\rho \left[ \frac{q^\beta p^\nu}{m_D^2 - m_\rho^2} - L^{\rho^+} \frac{g^{\beta\nu}}{2} (q^2 - m_\rho^2) \right] \\
& + M^{D^+} g_\rho \sqrt{m_D} \left[ \alpha_1 g^{\beta\nu} - \left( \alpha_1 - \alpha_2 \frac{q \cdot p}{m_D^2} \right) \frac{q^\beta q^\nu}{m_{V_0}^2} - \alpha_2 \frac{q^\beta p^\nu}{m_D^2} \right] \\
& + \frac{N}{\sqrt{2}} \tilde{g}_V \sqrt{m_D} \frac{a_2 \sin \theta_C \cos \theta_C}{f_{Cab}} \left[ \alpha_1 g^{\beta\nu} - \alpha_2 \frac{q^\beta p^\nu}{m_D^2} \right], \\
A_{PC}(D_s^+ \rightarrow K^{*+} l^+ l^-) &= 4J^{D_s^+} g_{K^*} f_{D_s^*} \sqrt{\frac{m_{D_s^*}}{m_{D_s}} \frac{m_{D_s^*}}{m_{K^*}^2 - m_{D_s^*}^2}} - 2K^{K^{*+}} C_{VV\Pi} f_{D_s} m_{D_s}^2 \\
& - \sqrt{2} N f_{D_s^*} \lambda \tilde{g}_V \frac{a_2 \sin \theta_C \cos \theta_C}{f_{Cab}} \sqrt{\frac{m_{D_s^*}}{m_{D_s}} \frac{m_{D_s^*}}{q^2 - m_{D_s^*}^2}}, \\
A_{PV}^{\beta\nu}(D_s^+ \rightarrow K^{*+} l^+ l^-) &= 2f_{D_s} g_{K^*} \left[ \frac{q^\beta p^\nu}{m_{D_s}^2 - m_{K^*}^2} - L^{K^{*+}} \frac{g^{\beta\nu}}{2} (q^2 - m_{K^*}^2) \right] \\
& + M^{D_s^+} g_{K^*} \sqrt{m_{D_s}} \left[ \alpha_1 g^{\beta\nu} - \left( \alpha_1 - \alpha_2 \frac{q \cdot p}{m_{D_s}^2} \right) \frac{q^\beta q^\nu}{m_{V_0}^2} - \alpha_2 \frac{q^\beta p^\nu}{m_{D_s}^2} \right] \\
& + \frac{N}{\sqrt{2}} \tilde{g}_V \sqrt{m_{D_s}} \frac{a_2 \sin \theta_C \cos \theta_C}{f_{Cab}} \left[ \alpha_1 g^{\beta\nu} - \alpha_2 \frac{q^\beta p^\nu}{m_{D_s}^2} \right], \\
A_{PC}(D^+ \rightarrow K^{*+} l^+ l^-) &= 4J^{D^+} g_{K^*} f_{D^*} \sqrt{\frac{m_{D^*}}{m_D} \frac{m_{D^*}}{m_{K^*}^2 - m_{D^*}^2}} - 2K^{K^{*+}} C_{VV\Pi} f_D m_D^2, \\
A_{PV}^{\beta\nu}(D^+ \rightarrow K^{*+} l^+ l^-) &= 2f_D g_{K^*} \left[ \frac{q^\beta p^\nu}{m_D^2 - m_{K^*}^2} - L^{K^{*+}} \frac{g^{\beta\nu}}{2} (q^2 - m_{K^*}^2) \right] \\
& + M^{D^+} g_{K^*} \sqrt{m_D} \left[ \alpha_1 g^{\beta\nu} - \left( \alpha_1 - \alpha_2 \frac{q \cdot p}{m_D^2} \right) \frac{q^\beta q^\nu}{m_{V_0}^2} - \alpha_2 \frac{q^\beta p^\nu}{m_D^2} \right],
\end{aligned}$$

$$\begin{aligned}
A_{PC}(D^0 \rightarrow K^{*0}l^+l^-) &= 4J^{D^0} g_{K^*} f_{D^*} \sqrt{\frac{m_{D^*}}{m_D}} \frac{m_{D^*}}{m_{K^*}^2 - m_{D^*}^2} - 2K^{\bar{K}^*0} C_{VV\Pi} f_D m_D^2, \\
A_{PV}^{\beta\nu}(D^0 \rightarrow K^{*0}l^+l^-) &= M^{D^0} g_{K^*} \sqrt{m_D} \left[ \alpha_1 g^{\beta\nu} - (\alpha_1 - \alpha_2) \frac{q \cdot p}{m_D^2} \frac{q^\beta q^\nu}{m_{V_0}^2} - \alpha_2 \frac{q^\beta p^\nu}{m_D^2} \right],
\end{aligned} \tag{26}$$

Here  $q = p_- + p_+$  and  $m_{V_0}$  can be approximately taken as the average of the  $\phi$ ,  $\omega$  and  $\rho$  masses. The coefficients  $J^D$ ,  $K^V$ ,  $L^V$ ,  $M^D$  and  $N$  are expressed as

$$\begin{aligned}
J^{D^0} &= \lambda' - \frac{\lambda \tilde{g}_V}{2\sqrt{2}} \left[ \frac{g_\rho}{q^2 - m_\rho^2 + i\Gamma_\rho m_\rho} + \frac{g_\omega}{3(q^2 - m_\omega^2 + i\Gamma_\omega m_\omega)} \right], \\
J^{D^+} &= \lambda' - \frac{\lambda \tilde{g}_V}{2\sqrt{2}} \left[ -\frac{g_\rho}{q^2 - m_\rho^2 + i\Gamma_\rho m_\rho} + \frac{g_\omega}{3(q^2 - m_\omega^2 + i\Gamma_\omega m_\omega)} \right], \\
J^{D_s^+} &= \lambda' + \frac{\lambda \tilde{g}_V}{2\sqrt{2}} \frac{2g_\phi}{3(q^2 - m_\phi^2 + i\Gamma_\phi m_\phi)}, \\
K^{\bar{K}^*0} &= \left[ \frac{g_\rho}{q^2 - m_\rho^2 + i\Gamma_\rho m_\rho} - \frac{g_\omega}{3(q^2 - m_\omega^2 + i\Gamma_\omega m_\omega)} + \frac{2g_\phi}{3(q^2 - m_\phi^2 + i\Gamma_\phi m_\phi)} \right] \frac{1}{m_D^2 - m_K^2}, \\
K^{K^{*+}} &= \left[ -\frac{g_\rho}{q^2 - m_\rho^2 + i\Gamma_\rho m_\rho} - \frac{g_\omega}{3(q^2 - m_\omega^2 + i\Gamma_\omega m_\omega)} + \frac{2g_\phi}{3(q^2 - m_\phi^2 + i\Gamma_\phi m_\phi)} \right] \frac{1}{m_D^2 - m_K^2}, \\
K^{\rho^+} &= -\frac{2g_\omega}{3(q^2 - m_\omega^2 + i\Gamma_\omega m_\omega)} \frac{1}{m_D^2 - m_\pi^2}, \\
K^{\rho^0} &= -2\sqrt{2} \frac{g_\rho}{q^2 - m_\rho^2 + i\Gamma_\rho m_\rho} \left[ \frac{f_{1mix}(f_{1mix} - f_{2mix})}{m_D^2 - m_{\eta^2}} + \frac{f'_{1mix}(f'_{1mix} - f'_{2mix})}{m_D^2 - m_{\eta'}} \right], \\
&\quad + \frac{\sqrt{2}}{3} \frac{g_\omega}{(q^2 - m_\omega^2 + i\Gamma_\omega m_\omega)} \frac{1}{m_D^2 - m_\pi^2}, \\
K^\omega &= -2\sqrt{2} \frac{g_\omega}{q^2 - m_\omega^2 + i\Gamma_\omega m_\omega} \left[ f_{1mix}(f_{1mix} - f_{2mix}) \text{ over } m_D^2 - m_{\eta^2} + \frac{f'_{1mix}(f'_{1mix} - f'_{2mix})}{m_D^2 - m_{\eta'}} \right], \\
&\quad + \sqrt{2} \frac{g_\rho}{q^2 - m_\rho^2 + i\Gamma_\rho m_\rho} \frac{1}{m_D^2 - m_\pi^2}, \\
K^\phi &= \frac{4}{3} \frac{g_\phi}{(q^2 - m_\phi^2 + i\Gamma_\phi m_\phi)} \left[ \frac{f_{1mix}(f_{1mix} - f_{2mix})}{m_D^2 - m_{\eta^2}} + \frac{f'_{1mix}(f'_{1mix} - f'_{2mix})}{m_D^2 - m_{\eta'}} \right], \\
L^{\rho^+} &= \frac{1}{q^2 - m_\rho^2 + i\Gamma_\rho m_\rho}, \\
L^{K^{*+}} &= \frac{1}{2g_{K^+}} \left( \frac{g_\rho}{q^2 - m_\rho^2 + i\Gamma_\rho m_\rho} + \frac{g_\omega}{3(q^2 - m_\omega^2 + i\Gamma_\omega m_\omega)} + \frac{2g_\phi}{3(q^2 - m_\phi^2 + i\Gamma_\phi m_\phi)} \right), \\
M^{D^0} &= \frac{g_\rho}{q^2 - m_\rho^2 + i\Gamma_\rho m_\rho} + \frac{g_\omega}{3(q^2 - m_\omega^2 + i\Gamma_\omega m_\omega)}, \\
M^{D^+} &= -\frac{g_\rho}{q^2 - m_\rho^2 + i\Gamma_\rho m_\rho} + \frac{g_\omega}{3(q^2 - m_\omega^2 + i\Gamma_\omega m_\omega)}, \\
M^{D_s^+} &= -\frac{2g_\phi}{3(q^2 - m_\phi^2 + i\Gamma_\phi m_\phi)},
\end{aligned} \tag{27}$$

and

$$N = \frac{g_\rho^2}{q^2 - m_\rho^2 + i\Gamma_\rho m_\rho} - \frac{g_\omega^2}{3(q^2 - m_\omega^2 + i\Gamma_\omega m_\omega)} - \frac{2g_\phi^2}{3(q^2 - m_\phi^2 + i\Gamma_\phi m_\phi)}. \quad (28)$$

The functions  $f_{1mix}$ ,  $f'_{1mix}$ ,  $f_{2mix}$  and  $f'_{2mix}$  are defined by

$$\begin{aligned} f_{1mix} &= \frac{f_\eta}{\sqrt{8}} \left[ \frac{1+c^2}{f_\eta} + \frac{sc}{f_{\eta'}} \right], & f'_{1mix} &= \frac{f_{\eta'}}{\sqrt{8}} \left[ \frac{sc}{f_\eta} + \frac{1+s^2}{f_{\eta'}} \right], \\ f_{2mix} &= \frac{f_\eta}{\sqrt{8}} \left[ \frac{1-5c^2}{f_\eta} - \frac{5sc}{f_{\eta'}} \right] & \text{and} & \quad f'_{2mix} = \frac{f_{\eta'}}{\sqrt{8}} \left[ \frac{-5sc}{f_\eta} + \frac{1-5s^2}{f_{\eta'}} \right], \end{aligned} \quad (29)$$

where  $s = \sin \theta_P$ ,  $c = \cos \theta_P$  and  $\theta_P \sim 20^\circ$  is the  $\eta - \eta'$  mixing angle. The values of the masses, decay constants and decay widths used are given in Table 2.

$H$	$m_H$	$f_H$	$P$	$m_P$	$f_P$	$V$	$m_V$	$g_V$	$\Gamma_V$
$D$	1.87	$0.21 \pm 0.04$	$\pi$	0.14	0.13	$\rho$	0.77	0.17	0.15
$D_s$	1.97	$0.24 \pm 0.04$	$K$	0.50	/	$K^*$	0.89	0.19	/
$D^*$	2.01	$0.21 \pm 0.04$	$\eta$	0.55	$0.13 \pm 0.008$	$\omega$	0.78	0.15	0.0084
$D_s^*$	2.11	$0.24 \pm 0.04$	$\eta'$	0.96	$0.11 \pm 0.007$	$\phi$	1.02	0.24	0.0044

Table 2: The pole masses  $m$ , decay constants  $f$  and decay widths  $\Gamma$  in  $GeV$ ; the constants  $g_V$  in  $GeV^2$ .

## ACKNOWLEDGMENTS

The research of S.F. and S.P. was supported in part by the Ministry of Science of the Republic of Slovenia. The research of P.S. was supported in part by the Fund for Promotion of Research at the Technion. One of us (S.F.) thanks the Physics Department at the Technion for the warm hospitality during her stay there, where part of this work was done. S. F. and S. P. are very grateful to G. Kernel and B. Kerševan for many useful discussions.

## Figure Captions

**Fig. 1.** Skeleton diagrams of various *long distance contributions* to the decay  $D \rightarrow Vl^+l^-$  resulting from Eq. (2). The spectator diagrams of type  $A_{Spec,\gamma}$  (see Eq. (2)) are shown in Fig. 1a, the spectator diagrams of type  $A_{Spec,V}$  are shown in Fig. 1b and the weak annihilation diagrams  $A_{Annih}$  are shown in Fig. 1c. Different diagrams are denoted by the roman numbers  $I - VIII$ . The square in each diagram denotes the weak transition due to the long distance Lagrangian  $\mathcal{L}_{LD}$  (Eq. 1). This Lagrangian contains a product of two weak currents, each denoted by a dot.

**Fig. 2.** Skeleton diagrams of *short distance contributions* to the decay  $D \rightarrow Vl^+l^-$  due to  $c \rightarrow ul^+l^-$  transition. The squares in the diagrams denote the weak transition due to the short distance Lagrangian  $\mathcal{L}_{SD}$  (Eq. 3). This Lagrangian contains a product of a quark and a lepton weak currents, each denoted by a dot.

**Fig. 3.** The differential branching ratio  $(1/\Gamma_D)d\Gamma(D^0 \rightarrow \bar{K}^{*0}\mu^+\mu^-)/dq^2$  as a function of  $q^2$  ( $q^2$  the invariant  $\mu^+\mu^-$  mass). The full line corresponds to the total branching ratio, while the dashed line represents the nonresonant long distance part. In the calculation the model parameters  $\lambda' = 0.26$  and  $C_{VV\Pi} = 0.31$  were used.

**Fig. 4.** The differential branching ratio  $(1/\Gamma_D)d\Gamma(D_s^+ \rightarrow \rho^+\mu^+\mu^-)/dq^2$  as a function of  $q^2$  ( $q^2$  the invariant  $\mu^+\mu^-$  mass). The full line corresponds to the total branching ratio, while the dashed line represents the nonresonant long distance part. In the calculation the model parameters  $\lambda' = 0.26$  and  $C_{VV\Pi} = 0.31$  were used.

**Fig. 5** The differential branching ratio  $(1/\Gamma_D)d\Gamma(D^0 \rightarrow \rho^0\mu^+\mu^-)/dq^2$  as a function of  $q^2$  ( $q^2$  the invariant  $\mu^+\mu^-$  mass). The full line represents to the total branching ratio, the dot-dashed line represents the short distance part, while the dashed line represents the nonresonant long distance part. In the calculation the model parameters  $\lambda' = 0.26$  and  $C_{VV\Pi} = 0.31$  were used.

**Fig. 6** The differential branching ratio  $(1/\Gamma_D)d\Gamma(D_s^+ \rightarrow K^{*+}\mu^+\mu^-)/dq^2$  as a function of  $q^2$  ( $q^2$  the invariant  $\mu^+\mu^-$  mass). The full line represents to the total branching ratio, the dot-dashed line represents the short distance part, while the dashed line represents the nonresonant long distance part. In the calculation the model parameters  $\lambda' = 0.26$  and  $C_{VV\Pi} = 0.31$  were used.

## References

- [1] I.I. Bigi, hep-ph/9408235.
- [2] J. L. Hewett, Report No. SLAC-PUB-95-6821 (unpublished).
- [3] S. Pakvasa, Report No. UH-511-871-97, to appear in Proc. of the FCNC 97 Conference, Santa Monica, CA, Feb. 1997 (to be published).
- [4] A. J. Schwartz, Mod. Phys. Lett. **A 8**, 967 (1993).
- [5] G.L. Castro, R. Martinez, J. H. Munoz, hep-ph/9804368, to be published in Phys. Rev. **D 58**, 033003 (1998).
- [6] K. S. Babu, X. G. He, X. -Q. Li, and S. Pakvasa, Phys. Lett. **B 205**, 540 (1988).
- [7] P. Singer and D.X. Zhang, Phys. Rev. **D 55**, R1127 (1997).
- [8] G. Burdman, E. Golowich, J. L. Hewett and S. Pakvasa, Phys. Rev. **D 52**, 6383 (1995).
- [9] S. Fajfer and P. Singer, Phys. Rev. **D 56**, 4302 (1997).
- [10] S. Fajfer, S. Prelovšek and P. Singer, hep-ph/9801279, to be published in Eur. Phys. J.C.
- [11] G. Greub, T. Hurth, M. Misiak and D. Wyler, Phys. Lett. **B 382**, 415 (1996).
- [12] B. Bajc, S. Fajfer and R. J. Oakes, Phys. Rev. **D 54**, 5883 (1996).
- [13] CLEO collaboration, A. Freyberger *et al.*, Phys. Rev. Lett. **76**, 3065 (1996); E653 collaboration, K. Kodama *et al.*, Phys. Lett. **B 345**, 82 (1995).
- [14] Particle Data Group, M. Barnett et al., Phys. Rev. **D 54**, 1 (1996).
- [15] M. Bauer, B. Stech and M. Wirbel, Z. Phys. **C 34**, 103 (1987).
- [16] B. Bajc, S. Fajfer and R. J. Oakes, Phys. Rev. **D 53**, 4957 (1996).
- [17] B. Bajc, S. Fajfer and R.J. Oakes, Phys. Rev. **D 51**, 2230 (1995).
- [18] R. Casalbuoni et al., Phys. Rep. **281**, 145 (1997) and references therein.
- [19] P. Singer and D. X. Zhang, Phys. Rev **D 54**, 1225 (1996).

- [20] B. Bajc, S. Fajfer, R. J. Oakes, S. Prelovšek, Phys. Rev. D **56**, 7207 (1997).
- [21] N. Isgur and M.B. Wise, Phys. Lett. **B 232**, 113 (1989); Phys. Lett. **B 237**, 527 (1990).
- [22] H. Georgi, Phys. Lett. **B 240**, 447 (1990).
- [23] M.B. Wise, Phys. Rev. **D 45**, 2188 (1992).
- [24] G. Burdman and J.F. Donoghue, Phys. Lett. **B 280**, 287 (1992).
- [25] T.M. Yan et al., Phys. Rev. **D 46**, 1148 (1992).
- [26] R. Casalbuoni et al., Phys. Lett. **B 292**, 371 (1992); R. Casalbuoni et al., Phys. Lett. **B 299**, 139 (1993).
- [27] N.G. Deshpande, X.G. He and J. Trampetic, Phys. Lett. **B 367**, 362 (1996); G. Eilam, A. Ioanissian, R.R. Mendel and P. Singer, Phys. Rev. **D 53**, 3629 (1996).
- [28] T. Inami and C. S. Lim, Prog. Theor. Phys. **65**, 197 (1981).
- [29] R. Safadi and P. Singer, Phys. Rev. **D 37**, 697 (1988); **42**, 1856(E) (1990); C.O. Dib, I. Dunietz and F.J. Gilman, Phys. Rev. **D 39**, 2639 (1989).
- [30] M. Bando, T. Kugo, S. Uehara, K. Yamawaki and T. Yanagida, Phys. Rev. Lett. **54**, 1215 (1985); M. Bando, T. Kugo, and K. Yamawaki, Nucl. Phys. B **259**, 493 (1985); Phys. Rep. 164, 217 (1988); T. Fujiwara, T. Kugo, H. Terao, S. Uehara, and K. Yamawaki, Prog. Th. Phys. **73**, 926 (1985).
- [31] E. Witten, Nucl. Phys. B **223**, 422 (1983).

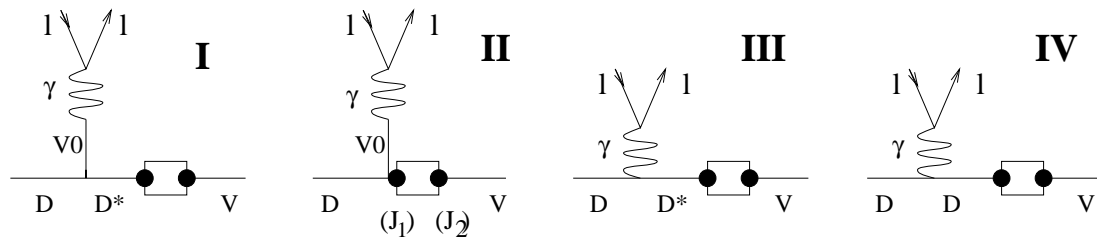


Fig. 1a

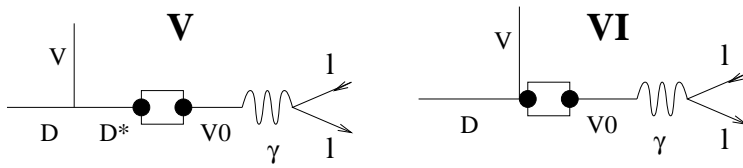


Fig. 1b

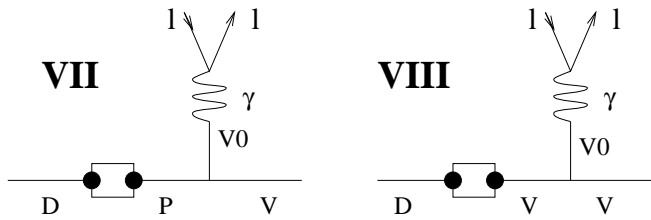


Fig. 1c

Fig. 1

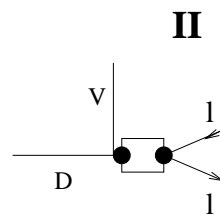
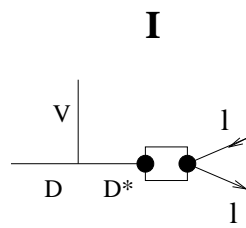


Fig. 2



Fig. 3

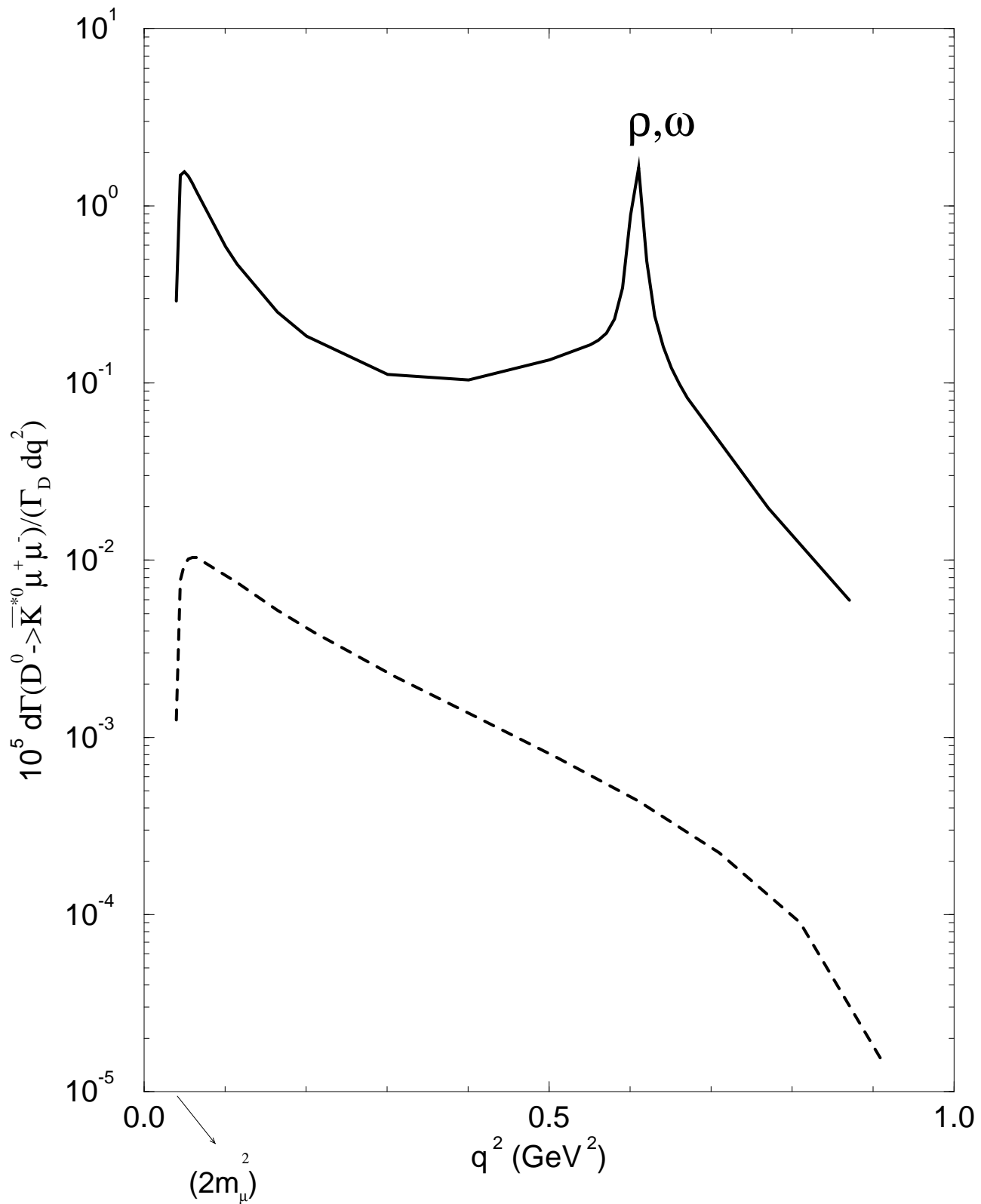


Fig. 4

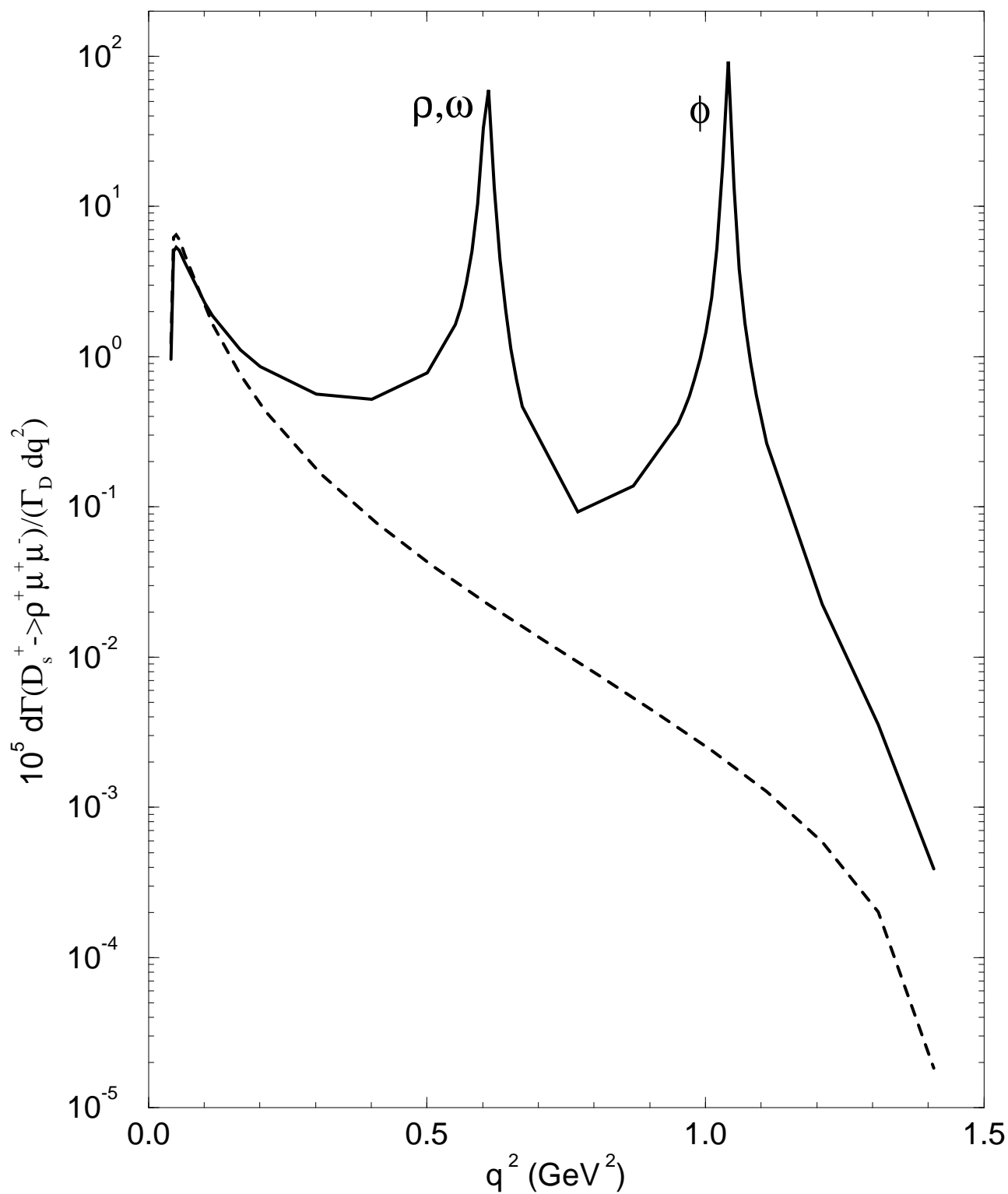


Fig. 5

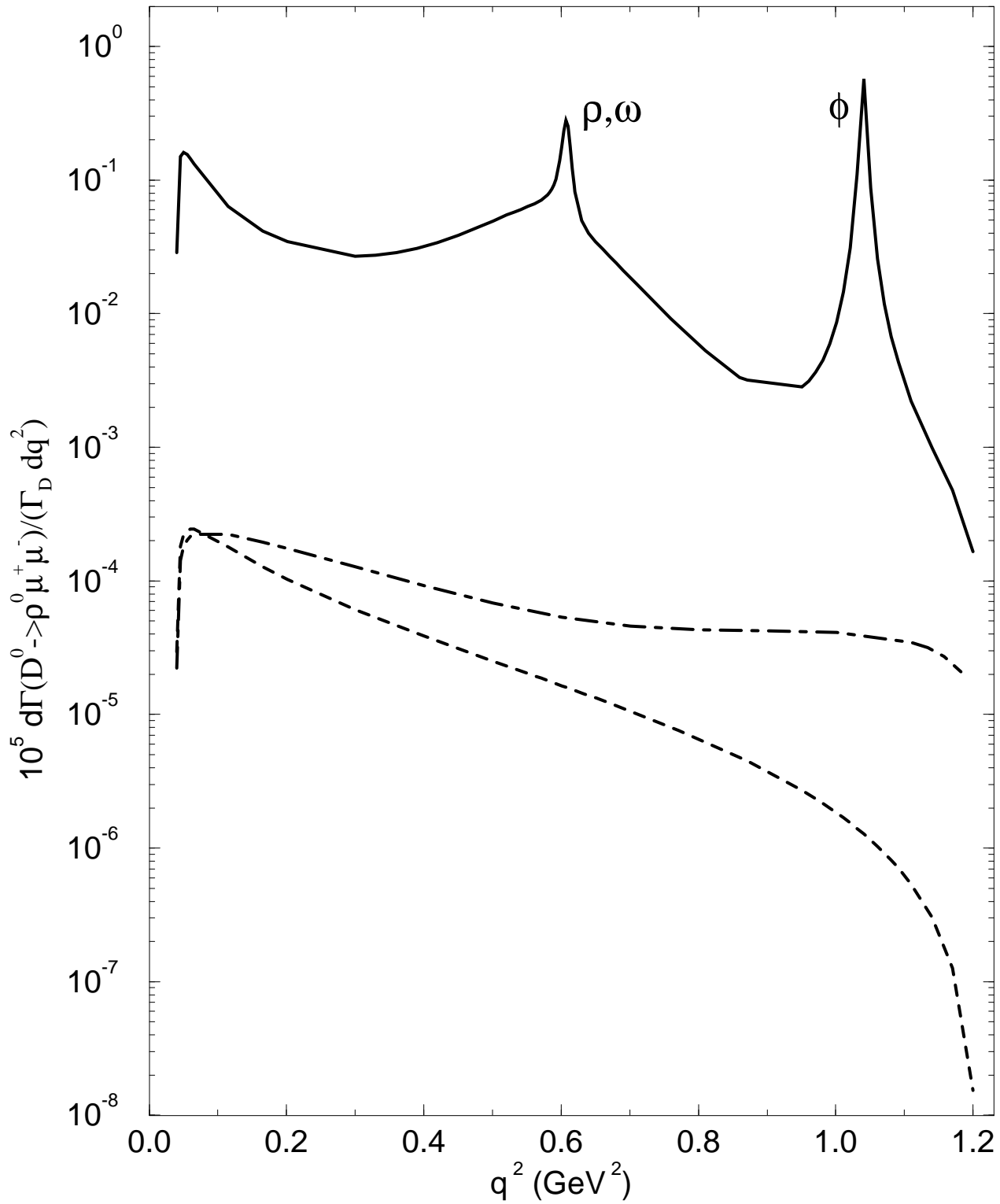


Fig. 6

